PAPER

Facile immobilization of gold nanoparticles into electrospun polyethyleneimine/polyvinyl alcohol nanofibers for catalytic applications†

Xu Fang,[ab] Hui Ma,[b] Shili Xiao,[c] Mingwu Shen,[b] Rui Guo,[b] Xueyan Cao[b] and Xiangyang Shi*[abd]

We report a facile approach to immobilizing gold nanoparticles (AuNPs) into electrospun polyethyleneimine (PEI)/polyvinyl alcohol (PVA) nanofibers for catalytic applications. In this study, electrospun PEI/PVA nanofibers with a mean diameter of 490 nm were first crosslinked with glutaraldehyde vapor to render them water stable. Then, the water-insoluble nanofibrous mats were used as nanoreactors to complex $AuCl_4^-$ anions *via* binding with the free amine groups of PEI for subsequent formation and immobilization of AuNPs. The formed AuNPs with a diameter of 11.8 nm within the nanofibers do not significantly change the morphology of the nanofibers; while importantly the mechanical property of the fibers was greatly improved compared to the crosslinked fibers without AuNPs. Scanning electron microscopy, Fourier transform infrared spectroscopy, transmission electron microscopy, energy dispersive spectroscopy, and thermogravimetric analysis were used to characterize these hybrid nanofibers. Furthermore, we show that the AuNP-containing nanofibers display an excellent catalytic activity and reusability for the transformation of 4-nitrophenol to 4-aminophenol. The present approach to fabricating AuNP-containing nanofibers may be extended for producing other nanoparticle-containing composite nanofibrous materials for various applications in catalysis, sensing, and biomedical sciences.

Introduction

Metal nanoparticles (NPs) have received immense scientific and technological interest in the areas including but not limited to electronics, optics, imaging, catalysis, biology, and sensor technology.[1–6] To synthesize stable metal NPs, various nanoreactor systems such as micelles,[7,8] microemulsions,[9] microgels,[10] liposomes,[11] liquid crystals,[12] dendrimers,[5,13] and polyelectrolyte multilayers[14] have been used. In most of these systems, polymers play an important role to generate NPs with desired properties. Among the many investigated metal NPs, gold NPs (AuNPs) have proven to be one of the most promising catalysts.[15–17] Colloidal AuNPs dispersed in aqueous or non-aqueous media used for catalytic applications generally suffer difficulty within recovery and thus reuse, thereby limiting their catalytic applications.

Therefore, fabricating a catalytic AuNP system with desired recovery and longevity still remains a great challenge.

Electrospinning is a facile and low-cost method to fabricating continuous polymer, inorganic, and organic/inorganic hybrid fibers with a high surface area to volume ratio and a high porosity.[18,19] Many synthetic and natural polymers have been electrospun to form nanofibers with a small diameter ranging from tens of nanometers to a few microns for various applications in solar cells,[20] filtration,[21] environmental remediation,[22,23] biosensors,[24] protective clothing,[25] and tissue engineering scaffolds.[26,27] The electrospun fibrous mats bear a great advantage in terms of the recovery and easy handling of the materials. Generating NP-containing nanofibrous mats is expected to be important for the development of NP-based nanocatalyst systems. Compared with other high-surface area, high-porosity materials for catalytic applications, electrospun polymer nanofibrous materials are easy to make, and the fiber diameter can be controlled by varying the electrospinning parameters. More importantly, through selection and modification of the fiber components, 3-dimensional complex organic/inorganic hybrid functional materials can be fabricated.

Literature data show that AuNPs can be immobilized onto the nanofiber surfaces through interfacial self-assembly[28–31] or within the nanofibers *via* electrospinning the AuNPs-containing polymer solution.[32–34] In most of the circumstances, the AuNPs have to be prepared before the electrospinning process. The NP-containing nanofibers can also be formed through the

[a]State Key Laboratory for Modification of Chemical Fibers and Polymer Materials, Donghua University, Shanghai, 201620, People's Republic of China

[b]College of Chemistry, Chemical Engineering and Biotechnology, Shanghai, 201620, People's Republic of China. E-mail: xshi@dhu.edu.cn

[c]Key Laboratory of Green Processing and Functional Textiles of New Textile Materials, Ministry of Education, Wuhan Textile University, Wuhan, 430073, People's Republic of China

[d]CQM- Centro de Química da Madeira, Universidade da Madeira, Campus da Penteada, 9000-390 Funchal, Portugal

This journal is © The Royal Society of Chemistry 2011

J. Mater. Chem., 2011, **21**, 4493–4501 | 4493

electrospinning of a polymer and metal salt mixture solution, followed by chemical reduction or physical treatment.[35,36] For example, Han *et al.*[35] prepared conductive gold films assembled on the electrospun poly(methyl methacrylate) fibrous mats using an *in situ* reduction method combined with electroless plating. Son and coworkers[36] fabricated cellulose acetate (CA) nanofibers containing silver NPs by UV irradiation of nanofibers electrospun from a CA/silver nitrate mixture solution. Electrospun fibrous mats of acrylonitrile and acrylic acid copolymers (PAN-AA) containing palladium NPs were prepared *via* electrospinning from a mixture solution of PAN-AA/PdCl$_2$, followed by chemical reduction.[37] Only a few examples are related to the use of functional groups of the nanofibers to complex metal ions for subsequent NP formation.[31]

In our previous studies,[38,39] we used electrospun polyacrylic acid (PAA)/polyvinyl alcohol (PVA) nanofibers as a nanoreactor to immobilize zerovalent iron NPs into the continuous nanofibers for decoloration of dyed wastewater. The nanoreactor concept from this system mainly resides in the use of PAA polymer, which can bind metal cations with the PAA carboxyl residues through ionic exchange for subsequent reductive formation of metal NPs. It is anticipated that developing an amine-based polycationic polymer nanofiber reactor system would allow for the binding of metal anions for the formation of other metal NPs (*e.g.*, AuCl$_4^-$). Polyethyleneimine (PEI) that has abundant amine groups on the molecular chains should be an ideal polymer for the fabrication of a polycationic nanofiber reactor.

In this present study, we developed a facile method to immobilize AuNPs into PEI/PVA polymer nanofibers for catalytic applications. Electrospun PEI/PVA nanofibers were crosslinked *via* glutaraldehyde (GA) vapor to render the fibrous mats water stable. Then, AuNPs were synthesized and immobilized into the electrospun PEI/PVA nanofibers through *in situ* reduction of the AuCl$_4^-$ ions complexed with the water-stable nanofibrous mats. Scanning electron microscopy (SEM), transmission electron microscopy (TEM), energy dispersive spectroscopy (EDS), Fourier transform infrared (FTIR) spectroscopy, and thermal gravimetric analysis (TGA) were utilized to characterize the morphology and composition of the AuNP-containing nanofibers. The catalytic activity of the formed AuNP-containing hybrid nanofibrous mats was evaluated *via* the transformation of 4-nitrophenol to 4-aminophenol. To our knowledge, this is the first report related to the use of electrospun nanofibers as nanoreactors to synthesize and immobilize AuNPs for catalysis applications. The developed NP-containing nanofibers with a high surface area to volume ratio and a high porosity should be amenable for use as a highly efficient and recoverable catalyst system. Findings from this study also document a facile approach using electrospun nanofibers as a nanoreactor to fabricate other NP-containing fibrous materials for various applications in catalysis, sensing, and biomedical sciences.

Experimental

Materials

PEI (branched, Mw = 750 000, 50%) was purchased from Sigma-Aldrich. PVA (88% hydrolyzed, Mw = 88 000) was obtained from J&K chemical. Chloroauric acid (HAuCl$_4$) and GA (25%)

were purchased from Sinopharm Chemical Reagent Co., Ltd. (China). Water used in all experiments was purified using a Milli-Q Plus 185 water purification system (Millipore, Bedford, MA) with a resistivity higher than 18 MΩ cm. All other chemicals were of analytical grade.

### Preparation of water-stable PEI/PVA nanofibers

PEI/PVA nanofibers were fabricated by electrospinning a 12 wt% PEI/PVA mixture solution according to literature with slight modification.[40] Specifically, PVA solution was prepared by dissolving PVA powder into water at 80 °C for 3 h under magnetic stirring, then cooled down to room temperature and stored in fridge before use.

PEI and PVA solutions were mixed together under magnetic stirring overnight with a mass ratio of PEI/PVA equivalent to 1 : 3 to achieve a homogeneous solution. The freshly prepared polymer solution was pumped into a syringe with a needle having an inner diameter of 0.8 mm. The flow rate was controlled by a syringe pump (JZB-1800, Jian Yuan Medical Technology Co., Ltd., China) at 0.3 mL h^{-1}. The high voltage power supplier (BGG40/2, Institute of Beijing High voltage Technology, China) was connected to a nozzle by a high-voltage insulating wire with two clamps at the end. An aluminium board was used as the collector and was connected to the ground. The electrospinning setup can be found in our previous report.[41] The electrospinning voltage was kept at 18.6 kV, and the collection distance was set at 25 cm. Under the above fixed electrospinning conditions, a polymer jet was formed, then elongated and ultimately deposited onto the aluminium (Al) foil, forming the nanofibrous mats.

Freshly prepared PEI/PVA nanofibrous mats were crosslinked by GA vapor to render them water stable.[42] A Petri dish containing 20 mL of GA solution (25% in aqueous solution) was first placed into a vacuum desiccator, then the electrospun PEI/PVA nanofibrous mats on Al foil were covered onto the dish without dipping into the GA solution. Vacuum was applied for 24 h. Then the crosslinked nanofibrous mats on Al foil were withdrawn and immersed into water for 5 min. This process led to the spontaneous detachment of the fibrous mats from the Al foil. The free-standing fibrous mats were then washed 3 times with water to remove excess GA. The water stability of the crosslinked free-standing nanofibrous mats was examined by soaking the fibrous mats in water for a week.

Immobilization of AuNPs into PEI/PVA nanofibrous mats

The AuNPs were synthesized and immobilized into the nanofibrous mats through an *in situ* reduction approach according to literature with slight modification (Scheme 1).[43,44] In brief, GA vapor-crosslinked free-standing nanofibrous mats (4 × 4.5 cm^2, 20 mg) were immersed into an HAuCl$_4$ aqueous solution (0.5 mM, 20 mL) for 1 h to allow AuCl$_4^-$ ions to complex with available PEI amine groups through ionic exchange, followed by rinsing with water for three times to remove excess AuCl$_4^-$ ions. Then AuNPs were synthesized by reducing AuCl$_4^-$ complexed with nanofibrous mats with NaBH$_4$ (2 mM, 20 mL) for 2 h. The formed AuNP-containing nanofibrous mats were rinsed 3 times with water, followed by vacuum drying at room temperature for 24 h, and stored in a desiccator before use.
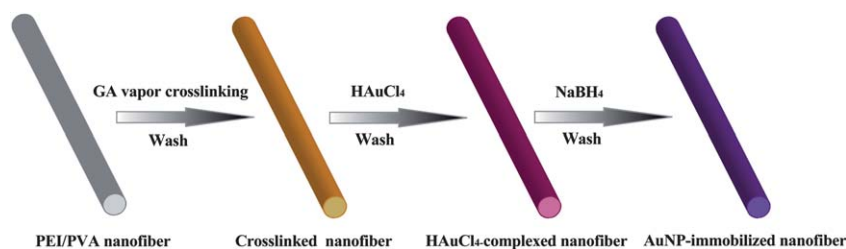
Scheme 1 Schematic illustration of the immobilization of AuNPs into electrospun PEI/PVA nanofibers.

Characterization

Morphologies of the electrospun PEI/PVA nanofibrous mats were observed using SEM (JSM-5600LV, JEOL Ltd., Japan) with an operating voltage of 15 kV. Prior to SEM measurements, samples were sputter-coated with 10 nm thick carbon films. The elemental composition of the samples was analyzed by EDS (IE300X, Oxford, U.K.) attached to the SEM. To observe the distribution of AuNPs in the nanofibers, the AuNP-immobilized polymer nanofibrous mats were embedded in epoxy resin and were cut into ultrathin sections with ultramicrotome equipped with a diamond knife. The cross-sectional image of the fibers containing AuNPs was imaged using a TEM (JEM2100, JEOL Ltd., Japan) with an operating voltage of 200 kV. The diameters of nanofibers and particle sizes were measured using image analysis software Image J 1.40G (http://rsb.info.nih.gov/ij/download.html). At least 300 randomly selected nanofibers or AuNPs in different SEM or TEM images were analyzed for each sample in order to acquire the diameter/size distribution histograms. TGA was carried out on a TG 209 F1 (NETZSCH Instruments Co., Ltd., Germany) thermogravimetric analyzer with a heating rate of 20 °C min^{-1} in air. FTIR spectra were recorded using a Nicolet 5700 spectrometer (Thermo Nicolet Corp.) at a wavenumber range of 3700–700 cm^{-1} under ambient conditions. The mechanical properties of the electrospun mats were examined using a materials testing machine (H5K-S, Hounsfield, UK) with an elongation speed of 10 mm min^{-1} at 20 °C and a relative humidity of 63%. Before measurements, 5 pieces of rectangular nanofibrous mats were cut into a dimension of 10 mm × 50 mm according to literature.[45] The apparent density and porosity of electrospun mats before and after treatment were calculated using eqn (1) and eqn (2),[46] where the thickness of the nanofibrous mats was measured by a micrometer.

$$\text{Apparent density (g cm}^{-3}) = \frac{\text{mat mass (g)}}{\text{mat thickness (cm)} \times \text{mat area (cm}^2)} \quad (1)$$

$$\text{Porosity} = \left\{ 1 - \frac{\text{mat apparent density (g cm}^{-3})}{\text{bulk density of mixture (g cm}^{-3})} \right\} \quad (2)$$

Catalysis experiments

The transformation of 4-nitrophenol to 4-aminophenol was performed to evaluate the catalytic efficiency and reusability of AuNP-containing PEI/PVA nanofibrous mats, similar to the procedure reported in the literature.[47,48] A mixture solution containing water (16.8 mL), 4-nitrophenol (0.6 mL, 10 mM), and NaBH$_4$ aqueous solution (0.6 mL, 10 M) was first prepared in a 25 mL glass beaker at room temperature, and then an AuNP-containing free-standing nanofibrous mat (20 mg, 3 × 4 cm^2) was immersed into the mixture solution, followed by gentle magnetic stirring. At each time interval, 0.5 mL of the aqueous solution was withdrawn and diluted to 1.5 mL for the analysis of transformation efficiency using a Lambda-25 UV-vis spectrometer (Perkin-Elmer, United States). The control experiment was carried out under similar conditions using the crosslinked free-standing PEI/PVA nanofibrous mats without AuNP immobilization. The other control experiment was also performed under similar conditions using PEI/PVA cast films with AuNP immobilization. The fabrication and charaterization of AuNP-containing PEI/PVA cast film can be seen in the Electronic Supplementary Information (ESI) (Fig. S1 and S2†). Note that for catalytic experiments, both AuNP-containing nanofibers and cast films had similar Au content. The transformation efficiency of 4-nitrophenol to 4-aminophenol was calculated according to eqn (3):

$$\text{Remaining fraction of 4 - nitrophenol} = \frac{C_t}{C_0} \times 100\% \quad (3)$$

where C_0 and C_t are the initial concentration of 4-nitrophenol and 4-nitrophenol concentration at a different time, respectively.

Results and discussion

Fabrication of water-stable electrospun PEI/PVA nanofibrous mats

To obtain uniform PEI/PVA nanofibers, we optimized the electrospinning parameters through variation of the flow rate, voltage, polymer concentration, and collection distance. Under the optimized experimental parameters (flow rate of 0.3 mL h^{-1}, voltage of 18.6 kV, collection distance of 25 cm, and polymer concentration of 12 wt%), smooth and uniform nanofibers with random orientation were generated with a mean diameter of 490 ± 83 nm (Fig. S3a†).

PEI/PVA nanofibrous mats thus prepared are water soluble, which is impractical for their subsequent catalytic applications in an aqueous environment. Therefore, the PEI/PVA nanofibers have to be crosslinked to render them water stable. The as-prepared nanofibers were crosslinked by GA vapor. The aldehyde groups of GA could interact with the amine groups of PEI and hydroxyl groups of PVA respectively, leading to the formation of water stable PEI/PVA nanofibrous mats. The

This journal is © The Royal Society of Chemistry 2011

J. Mater. Chem., 2011, **21**, 4493–4501 | 4495

morphology of the crosslinked PEI/PVA nanofibers was observed *via* SEM (Fig. 1a). It is clear that smooth and uniform fibrous structures are well retained, except for a slight increase in the mean diameter (592 ± 104 nm) when compared with that of the pristine nanofibers before crosslinking (490 ± 83 nm). This can be ascribed to the swelling of the fibers during the GA vapor crosslinking process.[42] We also noticed that the white color of PEI/PVA nanofibrous mats changed to yellowish after crosslinking, indicative of the formation of aldimine linkages between the free amino groups of PEI and the GA, in agreement with literature.[42] The morphology of crosslinked PEI/PVA nanofibers after immersing into water for a week was observed *via* SEM (Fig. S3b†). We showed that the porous fiber structures were well attained, further confirming the excellent water stability of the nanofibrous mats rendered *via* the GA vapor crosslinking method.

Synthesis and characterization of AuNP-containing PEI/PVA nanofibers

The available amine groups of PEI in the PEI/PVA nanofibers can be used to complex $AuCl_4^-$ anions *via* electrostatic interaction for subsequent formation of AuNPs, similar to the PAA/PVA fiber-based nanoreactor system reported in our previous studies.[38,39] Followed by immersing the $AuCl_4^-$ ion-containing free-standing fibrous mats into $NaBH_4$ solution, AuNPs were formed and simultaneously immobilized into the nanofibers (Scheme 1). A digital photograph clearly shows that after immobilization with AuNPs, the free standing fibrous mat becomes deep brown (Fig. S4 and S5†), suggesting the formation of AuNPs. SEM, TEM, FTIR, EDS, and TGA were used to characterize the AuNP-immobilized PEI/PVA nanofibrous mats.

SEM morphology observation shows that the AuNP-immobilized nanofibrous mats still retained a uniform porous fiber structure with a smooth surface (Fig. 1b), similar to the water stable electrospun PEI/PVA nanofibers without AuNPs (Fig. 1a). In the magnified SEM image of AuNP-immobilized nanofibers, some white dots distributed along the nanofibers

were clearly observed, which are believed to be the formed AuNPs (Fig. S6†). The mean diameter of the AuNP-containing nanofibers (675 ± 140 nm) was obviously larger than that of the PEI/PVA nanofibers without AuNPs, which might be caused by the swelling of the fibers after immersing into aqueous solution and the successful loading of the AuNPs.

Fig. 2 shows the cross-sectional TEM images of AuNP-containing PEI/PVA nanofibers and the size distribution histogram of the AuNPs formed in the nanofibers. Round-shaped patterns of AuNPs with a relatively uniform distribution are clearly observed, indicating that AuNPs are successfully formed along the cross section of the fibers (Fig. 2a). The mean size of AuNPs was estimated to be 11.8 ± 3.3 nm (Fig. 2c). Different from the uniform distribution of ZVI NPs (1.6 nm) in the PAA/PVA nanofibers observed in our previous studies,[38,39] we show that the distribution of AuNPs at the outer part of the fibers is much denser than that at the inner part of the fibers. This could be due to the lower concentration of $AuCl_4^-$ used to complex with the PEI/PVA nanofibers, thereby resulting in lower loading of the AuNPs. The lower loading percentage of AuNPs was also demonstrated by TGA results (see below). In addition, the lower mass ratio of PEI/PVA (1 : 3) compared with that of PAA/PVA (1 : 1) could also limit the binding of $AuCl_4^-$ ions for the formation of the densely distributed smaller AuNPs. High-resolution TEM images (Fig. 2b) of the individual AuNPs show that all AuNPs are crystalline, as lattices of Au crystals are clearly observed, in good agreement with literature.[49] EDS of the AuNP samples indicates the existence of Au elements (Fig. 3), demonstrating that the AuNPs were successfully immobilized into the nanofibers. The elemental oxygen can be attributed to the hydroxyl groups of the PVA polymer in the nanofibers. The elemental carbon detected was from the carbon coating and also from the main component of the polymer nanofibers. The chlorine signals were from the generated NaCl residue during the AuNP immobilization process.

Fig. 4 shows the FTIR spectra of PEI/PVA nanofibrous mats with different treatments. It is clear that there are still a considerable amount of primary amine groups available (1650 cm^{-1}) in the crosslinked PEI/PVA nanofibers, which is essential for the complexation of $AuCl_4^-$ anions. The peaks at 1600 cm^{-1} and 1050 cm^{-1} are indicative of the aldimine and ether linkages generated between GA/PEI and GA/PVA after crosslinking, respectively. The methylene groups for both PEI and PVA at 2940 cm^{-1} do not show significant variation after different treatments. The peaks of O–H and N–H stretching vibrations at 3350 cm^{-1} for the AuNP-containing nanofibers became broader than that of the PEI/PVA nanofibrous mats before and after crosslinking. This is presumably due to the interaction between the amino/hydroxyl groups of the PEI/PVA polymers and the immobilized AuNPs.

Porosity is one of the most important factors to evaluate the property of the nanofibrous mats before and after AuNP immobilization. Knowing the bulk densities of PEI and PVA polymers, along with the calculated apparent density of the nanofibers, we were able to calculate the porosities of PEI/PVA nanofibrous mats before and after crosslinking, and the AuNP-containing PEI/PVA nanofibrous mats (Table 1). The porosity of the PEI/PVA nanofibrous mats (51.62 ± 2.18%) prior to crosslinking increased to 65.54 ± 2.43% after GA vapor crosslinking,
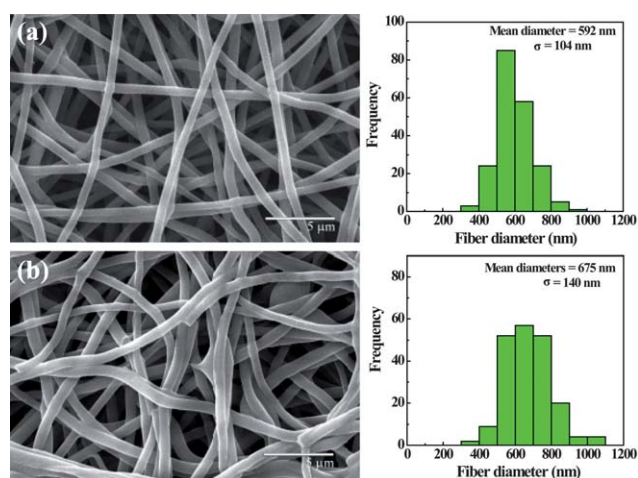

Fig. 1 SEM image and diameter distribution histogram of GA vapor-crosslinked PEI/PVA nanofibers (a) and AuNP-containing PEI/PVA nanofibers (b), respectively.
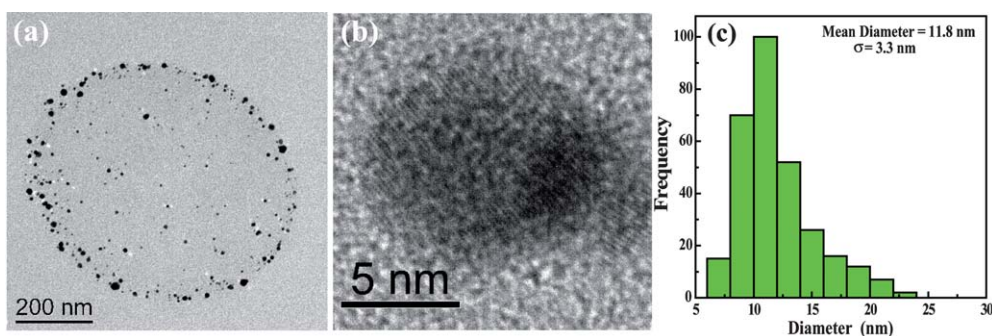
4496 | *J. Mater. Chem.*, 2011, **21**, 4493–4501

This journal is © The Royal Society of Chemistry 2011

Fig. 2 Cross-sectional TEM image (a) and high-resolution TEM image (b) of AuNP-containing PEI/PVA nanofibers; (c) shows the diameter distribution histogram of the immobilized AuNPs.
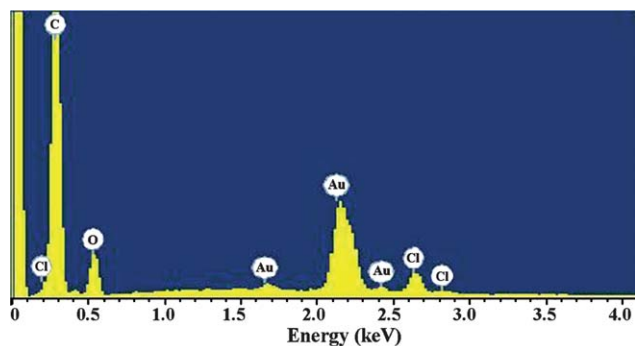

Fig. 3 EDS spectrum of the AuNP-containing electrospun polymer nanofibers.
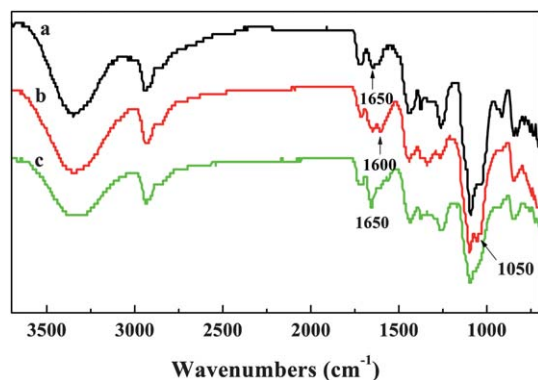

Fig. 4 FTIR spectra of the electrospun PEI/PVA nanofibers before (a) and after (b) GA vapor crosslinking; (c) shows the FTIR spectrum of AuNP-containing nanofibers.

which is presumably due to the swelling of the fibrous structure during the GA vapor crosslinking process. However, the porosity of AuNP-containing nanofibrous mats decreased to 41.48 ± 5.63%, which might be due to the loading of AuNPs into the nanofibers, causing a significant increase in the fiber diameter.

Mechanical properties are of paramount importance for the recovery and reuse of NP-containing fibrous materials used for practical catalytic applications. A typical tensile stress–strain curve of the electrospun PEI/PVA nanofibrous mats is shown in Fig. 5. Based on the stress–strain curves, the mechanical properties in terms of tensile stress, tensile strain, and the Young's

modulus are summarized in Table 2. It is clear that the tensile stress of the electrospun PEI/PVA nanofibrous mats (8.31 ± 1.25 MPa) before crosslinking increases to 9.84 ± 0.55 MPa after GA vapor crosslinking, which might be ascribed to the enhanced intermolecular interaction between the PEI and PVA during crosslinking, in agreement with literature data.[42] Meanwhile, the tensile stress of crosslinked PEI/PVA nanofibers improved greatly after the loading of AuNPs. However, the ultimate tensile strain of crosslinked PEI/PVA nanofibrous mats (35.60 ± 5.69%) and the AuNP-containing PEI/PVA nanofibers (35.26 ± 8.69%) displayed a large decrease when compared with PEI/PVA nanofibrous mats before crosslinking (133.6 ± 18.60%). This suggests that the crosslinking process makes the nanofibrous mats brittle. The Young's modulus of the nanofibrous mats after AuNPs immobilization (326.84 ± 59.94 MPa) was largely improved when compared with that of the nanofibrous mats with (162.48 ± 36.50 MPa) and without crosslinking (29.18 ± 9.12 MPa), which is presumably due to the load transfer from the polymer fibers to the immobilized AuNPs.

TGA was used to characterize the loading capacity of AuNPs immobilized into the water-stable PEI/PVA nanofibers (Fig. 6). At the high temperature of 900 °C, the polymer components were burnt out. The initial decrease of both nanofibers with and without AuNPs should be due to the loss of water in the fibers. The major weight loss within the region of 220–650 °C is attributed to the decomposition of the PEI/PVA polymers. The thermal decomposition temperatures were increased for the AuNP-containing fibrous mats in comparison with that of the nanofibrous mats without AuNPs, suggesting that the thermal stability of the hybrid nanofibrous mats is enhanced by the immobilization of AuNPs within the nanofibrous mats, in agreement with literature data.[50] We note that PEI/PVA nanofibrous mats with or without AuNPs all show an increased decomposition temperature compared to PEI/PVA cast films reported in the literature.[50] These results may be due to the fact that the high surface area to volume ratio of the nanofibrous

Table 1 Porosities of the electrospun PEI/PVA nanofibrous mats

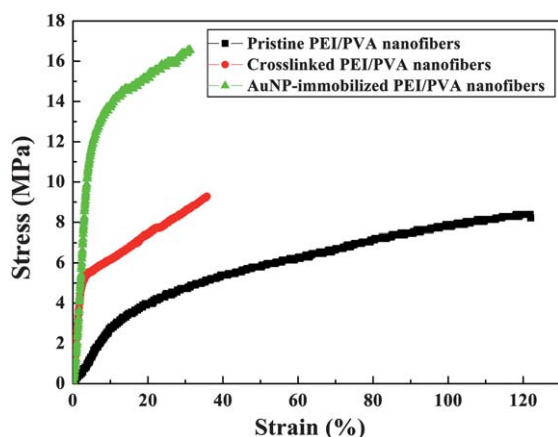| Nanofibrous mats	Apparent density (g cm^{-3})	Porosity (%)
Before crosslinking	0.60 ± 0.03	51.62 ± 2.18
After crosslinking	0.43 ± 0.03	65.54 ± 2.43
After AuNP immobilization	0.73 ± 0.07	41.48 ± 5.63

Fig. 5 Stress–strain curves of the pristine non-crosslinked electrospun PEI/PVA nanofibrous mats, the GA vapor-crosslinked PEI/PVA nanofibers, and the AuNP-immobilized PEI/PVA nanofibers.

Table 2 Mechanical properties of the PEI/PVA nanofibrous mats

Nanofibrous mats	Tensile stress (MPa)	Tensile strain (%)	Young's modulus (MPa)
Before crosslinking	8.31 ± 1.25	133.60 ± 18.60	29.18 ± 9.12
After crosslinking	9.84 ± 0.55	35.60 ± 4.69	162.48 ± 36.50
After AuNP immobilization	16.31 ± 0.57	35.26 ± 8.69	326.84 ± 59.94

materials makes the nanofibrous mats more heat resistant than the cast film with a significantly lower surface area. Based on the TGA data, the loading of the AuNPs in the nanofibrous mats was estimated to be 11.26%. It is interesting to note that the process of loading AuNPs within the nanofibers involves additional steps of exposing fiber membranes to an $HAuCl_4$ water solution, rinsing with water, reducing $AuCl_4^-$ ions within the fibers, and further rinsing with water, the final nanofibers may experience additional swelling. Therefore, the increase of the fiber diameter from 590 nm to 670 nm after AuNP immobilization cannot be solely correlated to the Au loading.

Catalytic reduction of 4-nitrophenol

To explore the potential catalytic applications of the AuNP-immobilized PEI/PVA nanofibrous mat, we selected a reaction to transform 4-nitrophenol to 4-aminophenol as a model. The reaction was monitored using UV-vis spectroscopy. We showed that the AuNP-immobilized nanofibrous mats were able to effectively catalyze the reaction to transform 4-nitrophenol to 4-aminophenol in the presence of $NaBH_4$ (Fig. 7a and 7b). It is clear that the yellow color of the 4-nitrophenol solution gradually faded with the reaction time (Fig. 7a), and the intensity of the characteristic absorption peak of 4-nitrophenol at 400 nm significantly decreased within the time frame of 36 min (Fig. 7b). It is also interesting to note that the characteristic absorption peaks are not interfered by the surface plasmon peak of the AuNPs (typically at 520 nm), indicating that the AuNPs immobilized within the nanofibrous mats are stable and do not leak from the mats. Meanwhile, the catalytic reduction of
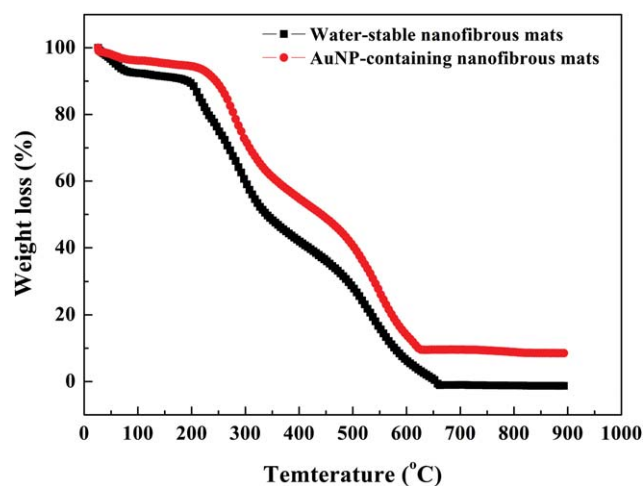

Fig. 6 TGA curves of the PEI/PVA nanofibers before and after AuNP immobilization.

4-nitrophenol can also be evidenced by the appearance of a new characteristic absorption peak at 300 nm possessed by the formed 4-aminophenol.[47] In contrast, when PEI/PVA nanofibrous mats without AuNPs were exposed to the same 4-nitrophenol solution, we did not observe significant decoloration of the 4-nitrophenol within 36 min. Only a slight decrease in the intensity of the absorption peak at 400 nm was observed (Fig. 7c), which should be due to the physical adsorption of the 4-nitrophenol onto the surface of the PEI/PVA nanofibrous mats. This further confirmed that the superior transformation of 4-nitrophenol to 4-aminophenol was solely related to the excellent catalytic property of the immobilized AuNPs.

The AuNP-immobilized PEI/PVA nanofibrous mat could be reusable and recyclable. The excellent catalytic activity of the AuNP-immobilized nanofibrous mats was also demonstrated by plotting the remaining fraction of 4-nitrophenol as a function of exposure time (Fig. 8). After catalyzing the 4-nitrophenol solution for the first time, the hybrid nanofibrous mats without any treatments still performed well for the second and third time catalysis experiment. The ultimate transformation efficiency of 4-nitrophenol to 4-aminophenol could be up to 97% at 36 min. It is worthwhile noting that the AuNPs immobilized within the PEI/PVA nanofibrous mats display excellent catalytic activity, primarily due to the high surface area to volume ratio and high porosity of the fibrous nanostructures that allow efficient contact of the AuNPs with the substrate molecules. In contrast, AuNPs immobilized within PEI/PVA cast films that were used to catalyze the transformation of 4-nitrophenol to 4-aminophenol under similar conditions had a lower catalytic activity (Fig. S7†). The transformation efficiency could only reach 72% at the same time point of 36 min. The lower catalytic activity of AuNP-immobilized cast films is likely due to the lower surface area to volume ratio and the lower porosity of the solid films when compared to those of the nanofibrous mats, leading to limited contact of AuNPs with the substrate molecules. Another reason could be that the AuNPs formed in the cast films had a certain degree of aggregation (Fig. S2†). In addition, we showed that the morphology of the nanofibers after catalyzing the reaction 3 times was well retained (Fig. S8†), further confirming the
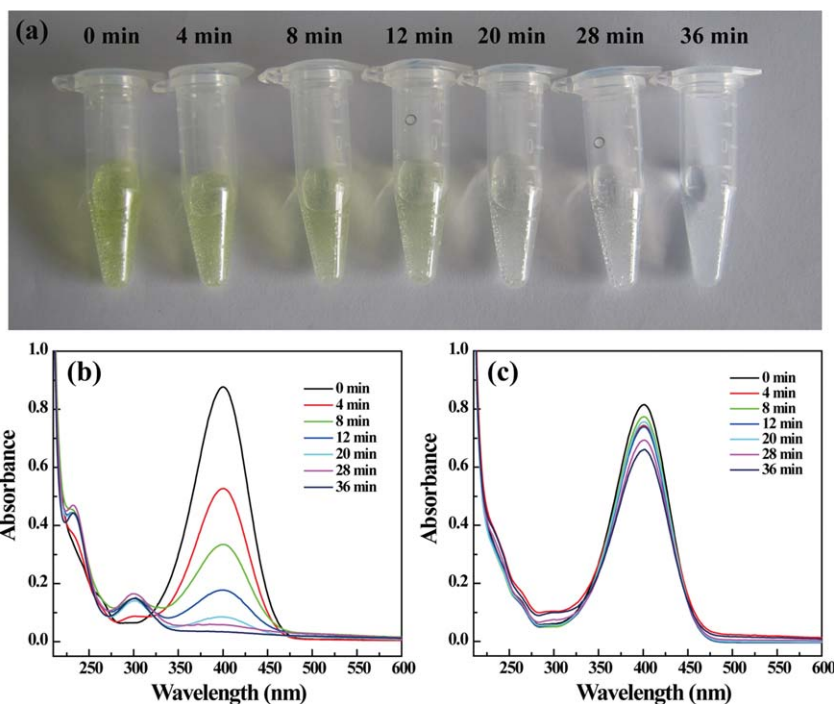
Fig. 7 Photograph of the 4-nitrophenol aqueous solution treated with the AuNP-containing nanofibers at different time intervals (a), and UV-vis spectra of 4-nitrophenol aqueous solution catalyzed with the AuNP-containing PEI/PVA nanofibrous mats (b) and treated with PEI/PVA nanofibrous mats without AuNPs (c) at different time intervals.
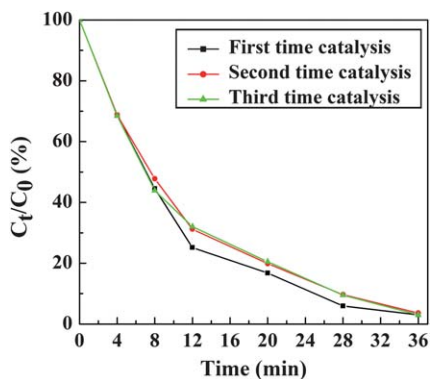

Fig. 8 The efficiency of the AuNPs-containing PEI/PVA nanofibrous mats to catalyze the transformation of 4-nitrophenol to 4-aminophenol for the first, second, and third time.

stability of the composite nanofibers in aqueous solution. The Au signals in the EDS spectrum (Fig. S9†) of the hybrid nanofibrous mats after being used 3 times further confirmed that the immobilized AuNPs are very stable and are not released from the nanofibrous mat during the catalytic reduction process. In general, when colloidal AuNPs are used as catalysts, the main difficulty is how to recycle the particles from the solution for 2nd and 3rd time catalysis. In our approach, the fabricated free-standing fibrous membrane with AuNPs immobilized can be easily recycled for further catalytic uses, thereby providing a cost-effective approach for catalytic applications.

For catalytic applications, the thermostability of the AuNPs immobilized within polymer nanofibers is important, as change in the temperature may introduce the aggregation and ripening of the particles, leading to decreased catalytic performance. To prove whether or not the immobilized AuNPs in the nanofibers are thermally stable, the AuNP-containing nanofibrous mats were heated to 50 °C, 80 °C, and 150 °C, respectively for 1 h. Although the photograph of the bulk nanofibrous mats did not show any appreciable changes at different temperatures (Fig. S10†), this did not give the exact information related to the size and morphology changes of the immobilized AuNPs. Therefore, TEM imaging of the sectioned nanofibrous mats treated at different temperatures was performed (Fig. 9). It is clear that the size of the AuNPs does not exhibit any appreciable changes, indicating that the AuNPs immobilized within the PEI/PVA nanofibers are pretty thermally stable. As opposed to AuNPs immobilized within the nanofibers without treatment or treated at lower temperature (50 °C) that were dominantly distributed at the outer part of the fiber cross section (Fig. 2 and 9), the heating treatment seems to drive the AuNPs to move to the central part of the fiber cross section, thus leading to a more uniform particle distribution. Furthermore, the AuNP-containing nanofibers treated at different temperatures were used to catalyze the transformation of 4-nitrophenol to 4-aminophenol (Fig. 10). We showed that the catalytic efficiency of AuNPs immobilized within the nanofibers did not have any changes when compared with that without heating treatment (Fig. 8). This further confirms that the AuNPs immobilized within the nanofibers are thermally stable at the studied temperature ranges, and the heating treatment does not compromise the excellent catalytic activity of the particles. Taken together, our results imply that the as-prepared hybrid nanofibrous mats are promising candidates for catalysis applications with high efficiency, high stability, and high reusability.
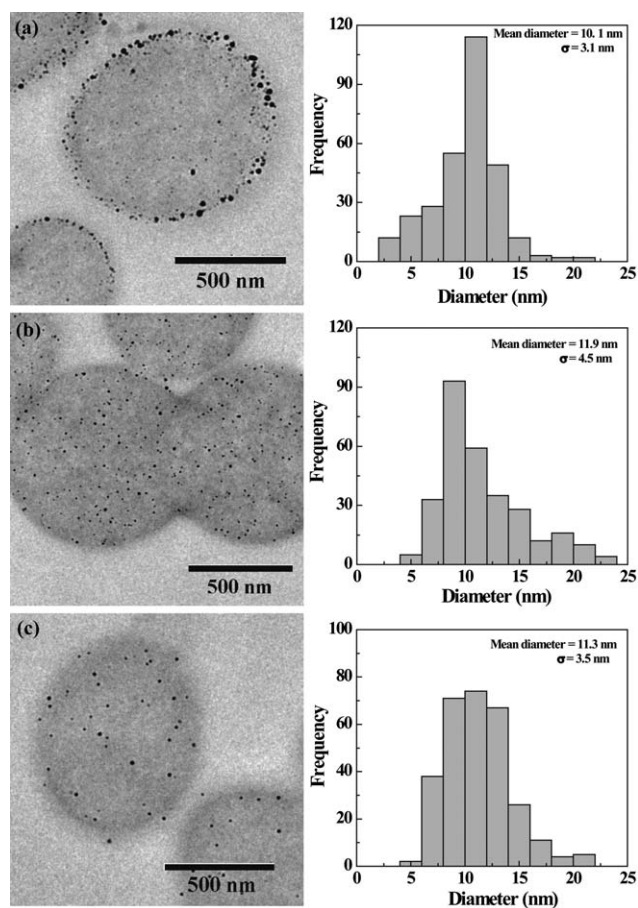
Fig. 9 TEM images of the AuNP-containing PEI/PVA nanofibrous mats after heating at (a) 50 °C, (b) 80 °C, and (c) 150 °C for 1 h.
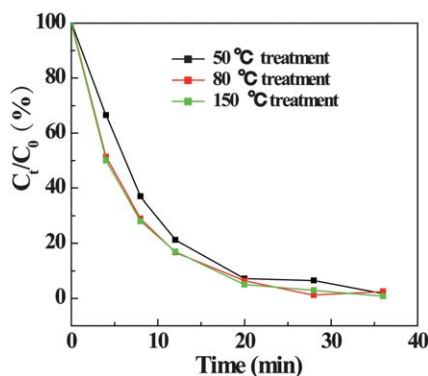

Fig. 10 The efficiency of thermally treated AuNP-containing PEI/PVA nanofibrous mats to catalyze the transformation of 4-nitrophenol to 4-aminophenol. (a) 50 °C, (b) 80 °C, and (c) 150 °C.

Conclusions

In summary, we developed a facile approach to simultaneously synthesizing and immobilizing AuNPs within PEI/PVA nanofibrous mats. The immobilization of the AuNPs with a mean diameter of 11.8 nm within the PEI/PVA nanofibers does not impact the porous fibrous structure of the mats. The AuNP-containing PEI/PVA nanofibers with a mean diameter of 675 nm

are very stable in water and have a porosity of 41.48 ± 5.63%. The catalytic reaction to transform 4-nitrophenol to 4-amino-phenol demonstrates that the AuNP-immobilized nanofibrous mats are able to catalyze the reaction with an efficiency approaching 97% within 36 min. Furthermore, the AuNP-immobilized PEI/PVA nanofibrous mats can be easily handled and reused for at least 3 times with similar catalytic performance. Given the unique features of the nanofiber-based reactor system, we anticipated that the loading percentage of AuNPs and the size of the AuNPs could be controlled by varying the mass ratio of PEI/PVA in the fibers, the initial concentration of the $HAuCl_4$ immersing solution, and the number of $AuCl_4^-$ anion complexation and reduction cycles.[51,52] This would provide a means to tune the catalytic activity of the AuNP-immobilized fibrous mats. The related work is currently underway in our laboratory. Furthermore, the developed PEI-based nanofiber nanoreactor system may be applicable for the immobilization of other metal or inorganic NPs for various applications in catalysis, sensing, and biomedical sciences.

Notes and references

1 A. N. Shipway, E. Katz and I. Willner, *ChemPhysChem*, 2000, **1**, 18–52.
2 P. Serp, M. Corrias and P. Kalck, *Appl. Catal., A*, 2003, **253**, 337–358.
3 S. H. Sun, S. Anders, T. Thomson, J. E. E. Baglin, M. F. Toney, H. F. Hamann, C. B. Murray and B. D. Terris, *J. Phys. Chem. B*, 2003, **107**, 5419–5425.
4 Y. G. Sun and Y. N. Xia, *Science*, 2002, **298**, 2176–2179.
5 X. Shi, S. Wang, S. Meshinchi, M. E. Van Antwerp, X. Bi, I. Lee and J. R. Baker, Jr, *Small*, 2007, **3**, 1245–1252.
6 M. C. Daniel and D. Astruc, *Chem. Rev.*, 2004, **104**, 293–346.
7 L. Samuelson, W. Liu, R. Nagarajan, J. Kumar, F. F. Bruno, A. Cholli and S. Tripathy, *Synth. Met.*, 2001, **119**, 271–272.
8 D. Ingert and M. P. Pileni, *Adv. Funct. Mater.*, 2001, **11**, 136–139.
9 L. Manziek, E. Langenmayr, A. Lamola, M. Gallagher, N. Brese and N. Annan, *Chem. Mater.*, 1998, **10**, 3101–3108.
10 Y. Lu, S. Proch, M. Schrinner, M. Drechsler, R. Kempe and M. Ballauff, *J. Mater. Chem.*, 2009, **19**, 3955–3961.
11 A. Graff, M. Winterhalter and W. Meier, *Langmuir*, 2001, **17**, 919–923.
12 T. M. Dellinger and P. V. Braun, *Scr. Mater.*, 2001, **44**, 1893–1897.
13 Y. M. Chung and H. K. Rhee, *Catal. Lett.*, 2003, **85**, 159–164.
14 X. Shi, M. Shen and H. Mohwald, *Prog. Polym. Sci.*, 2004, **29**, 987–1019.
15 A. S. K. Hashmi and G. J. Hutchings, *Angew. Chem., Int. Ed.*, 2006, **45**, 7896–7936.
16 B. Hvolbæk, T. V. W. Janssens, B. S. Clausen, H. Falsig, C. H. Christensen and J. K. Nørskov, *Nano Today*, 2007, **2**, 14–18.
17 G. C. Bond and D. T. Thompson, *Catal. Rev. Sci. Eng.*, 1999, **41**, 319–388.
18 D. Li and Y. N. Xia, *Adv. Mater.*, 2004, **16**, 1151–1170.

4500 | *J. Mater. Chem.*, 2011, **21**, 4493–4501

This journal is © The Royal Society of Chemistry 2011

19 D. H. Reneker and I. Chun, *Nanotechnology*, 1996, **7**, 216–223.
20 K. Fujihara, A. Kumar, R. Jose, S. Ramakrishna and S. Uchida, *Nanotechnology*, 2007, 18.
21 L. Lebrun, F. Vallee, B. Alexandre and Q. T. Nguyen, *Desalination*, 2007, **207**, 9–23.
22 K. Yoon, B. S. Hsiao and B. Chu, *J. Mater. Chem.*, 2008, **18**, 5326–5334.
23 H. Schreuder-Gibson, P. Gibson, K. Senecal, M. Sennett, J. Walker, W. Yeomans, D. Ziegler and P. P. Tsai, *J. Adv. Mater.*, 2002, **34**, 44–55.
24 X. Y. Wang, Y. G. Kim, C. Drew, B. C. Ku, J. Kumar and L. A. Samuelson, *Nano Lett.*, 2004, **4**, 331–334.
25 W. E. Teo and S. Ramakrishna, *Nanotechnology*, 2006, **17**, R89–R106.
26 K. H. Hong, *Polym. Eng. Sci.*, 2007, **47**, 43–49.
27 Z. W. Ma, M. Kotaki, R. Inai and S. Ramakrishna, *Tissue Eng.*, 2005, **11**, 101–109.
28 K. Muller, J. F. Quinn, A. P. R. Johnston, M. Becker, A. Greiner and F. Caruso, *Chem. Mater.*, 2006, **18**, 2397–2403.
29 B. Wang, B. Li, J. Xiong and C. Y. Li, *Macromolecules*, 2008, **41**, 9516–9521.
30 H. Dong, D. Wang, G. Sun and J. P. Hinestroza, *Chem. Mater.*, 2008, **20**, 6627–6632.
31 H. Dong, E. Fey, A. Gandelman and W. E. Jones, *Chem. Mater.*, 2006, **18**, 2008–2011.
32 J. Bai, Q. Yang, M. Li, S. Wang, C. Zhang and Y. Li, *Mater. Chem. Phys.*, 2008, **111**, 205–208.
33 W. Shi, W. Lu and L. Jiang, *J. Colloid Interface Sci.*, 2009, **340**, 291–297.
34 J. Bai, Y. X. Li, S. T. Yang, J. S. Du, S. G. Wang, J. F. Zheng, Y. Z. Wang, Q. B. Yang, X. S. Chen and X. B. Jing, *Solid State Commun.*, 2007, **141**, 292–295.
35 G. Y. Han, B. Guo, L. W. Zhang and B. S. Yang, *Adv. Mater.*, 2006, **18**, 1709–1712.
36 W. K. Son, J. H. Youk and W. H. Park, *Carbohydr. Polym.*, 2006, **65**, 430–434.
37 M. M. Demir, M. A. Gulgun, Y. Z. Menceloglu, B. Erman, S. S. Abramchuk, E. E. Makhaeva, A. R. Khokhlov, V. G. Matveeva and M. G. Sulman, *Macromolecules*, 2004, **37**, 1787–1792.
38 S. Xiao, M. Shen, R. Guo, S. Wang and X. Shi, *J. Phys. Chem. C*, 2009, **113**, 18062–18068.
39 S. Xiao, M. Shen, R. Guo, Q. Huang, S. Wang and X. Shi, *J. Mater. Chem.*, 2010, **20**, 5700–5708.
40 C. Dong, X. Yuan, M. He and K. Yao, *J. Biomater. Sci., Polym. Ed.*, 2006, **17**, 631–643.
41 F. J. Liu, R. Guo, M. W. Shen, S. Y. Wang and X. Y. Shi, *Macromol. Mater. Eng.*, 2009, **294**, 666–672.
42 Y. Zhang, J. Venugopal, Z. M. Huang, C. T. Lim and S. Ramakrishna, *Polymer*, 2006, **47**, 2911–2917.
43 M. M. Demir, G. Ugur, M. A. Gulgun and Y. Z. Menceloglu, *Macromol. Chem. Phys.*, 2008, **209**, 508–515.
44 J. Dai and M. L. Bruening, *Nano Lett.*, 2002, **2**, 497–501.
45 Z. M. Huang, Y. Z. Zhang, S. Ramakrishna and C. T. Lim, *Polymer*, 2004, **45**, 5361–5368.
46 W. He, Z. W. Ma, T. Yong, W. E. Teo and S. Ramakrishna, *Biomaterials*, 2005, **26**, 7606–7615.
47 K. Hayakawa, T. Yoshimura and K. Esumi, *Langmuir*, 2003, **19**, 5517–5521.
48 K. Esumi, R. Isono and T. Yoshimura, *Langmuir*, 2004, **20**, 237–243.
49 X. Shi, T. R. Ganser, K. Sun, L. P. Balogh and J. R. Baker, Jr, *Nanotechnology*, 2006, **17**, 1072–1078.
50 K. H. Wu, P. Y. Yu, Y. J. Hsieh, C. C. Yang and G. P. Wang, *Polym. Degrad. Stab.*, 2009, **94**, 2170–2177.
51 Q. Huang, X. Shi, R. A. Pinto, E. Petersen and W. J. Weber, Jr, *Environ. Sci. Technol.*, 2008, **42**, 8884–8889.
52 S. Xiao, S. Wu, M. Shen, R. Guo, Q. Huang, S. Wang and X. Shi, *ACS Appl. Mater. Interfaces*, 2009, **1**, 2848–2855.

This journal is © The Royal Society of Chemistry 2011

J. Mater. Chem., 2011, **21**, 4493–4501 | 4501